Available online at www.sciencedirect.com
ScienceDirect
Applied Catalysis B: Environmental 82 (2008) 273–283
APPLIED CATALYSIS B: ENVIRONMENTAL
www.elsevier.com/locate/apcatb

Studies on the activation of hydrogen peroxide for color removal in the presence of a new Cu(II)-polyampholyte heterogeneous catalyst

Juan Manuel Lázaro Martínez [a], María Florencia Leal Denis [b], Lidia Leonor Piehl [c], Emilio Rubín de Celis [c], Graciela Yolanda Buldain [a], Viviana Campo Dall' Orto [b,*]

[a] *Departamento de Química Orgánica, Facultad de Farmacia y Bioquímica, Universidad de Buenos Aires, Junín 956 (C1113AAD), Ciudad Autónoma de Buenos Aires, Argentina*
[b] *Departamento de Química Analítica y Fisicoquímica, Facultad de Farmacia y Bioquímica, Universidad de Buenos Aires, Junín 956 (C1113AAD), Ciudad Autónoma de Buenos Aires, Argentina*
[c] *Departamento de Físicomatemática, Facultad de Farmacia y Bioquímica, Universidad de Buenos Aires, Junín 956 (C1113AAD), Ciudad Autónoma de Buenos Aires, Argentina*

Received 19 December 2007; received in revised form 25 January 2008; accepted 30 January 2008
Available online 9 February 2008

Abstract

In this work we describe the application of a new non-soluble and non-porous complex with copper ion based on ethylene glycol diglycidyl ether (EGDE), methacrylic acid (MAA) and 2-methylimidazole (2MI) in the decolorization of an azo dye Methyl Orange (MO) as a model pollutant at room temperature.

The complex with copper ion was studied by ESR and SEM and was tested as a heterogeneous catalyst for H_2O_2 activation. A possible mechanism of interaction involves the production of hydroxyl radicals (confirmed by ESR), dioxygen and water.

The Cu(II)-polyampholyte/H_2O_2 system acted efficiently in the color removal of MO. The adsorption and oxidative degradation of the azo-based dye followed pseudo-first-order kinetic profiles, and the rate constant for degradation had a second-order dependence on copper ion content in the mixture.

A removal of MO higher than 90% was achieved in 20 min at pH 7.0, combining 0.8 mM of complexed copper ions in the mixture with 24 mM hydrogen peroxide.

The dye adsorbed on the polyampholyte following a L4-type isotherm with 4.9 μmol g^{-1} maximum loading capacity and 3.1 μM dissociation constant for the first monolayer.

Keywords: Heterogeneous catalyst; Copper ion; Hydrogen peroxide; Azo dyes; ESR

1. Introduction

One of the most serious environmental problems that the textile industry faces is the removal of color from the waste streams. Due to this stability of modern pigments, there is an increasing need of new physical, chemical or biological methods of treatment [1–6].

In general, dyes are either poorly biodegradable or resistant to environmental conditions [7]. Adsorption is considered to be relatively superior to other techniques because of its low cost, simplicity of design and availability and ability to treat dyes in more concentrated forms [8,9]. One of the most widely used adsorbent is the granular activated carbon for the removal of color in wastewater treatment industry. However, carbon adsorption continues to be an expensive and difficult process for this application [10,11].

Hydrogen peroxide is a powerful, non-specific oxidant adequate for degradation of pollutants that can be used in

Abbreviations: Cu(II), copper ion; Cu(II)-poly(EGDE-MAA-2MI), complex between copper ion and the polyampholyte obtained by reaction of ethylene glycol diglycidyl ether, methacrylic acid and 2-methylimidazole; MO, Methyl Orange; H_2O_2, hydrogen peroxide; ESR, electron spin resonance; DMPO, 5,5-dimethyl-1-pyrroline-*N*-oxide; FTIR, Fourier transform infra-red; SEM, scanning electron microscopy; **R**, coefficient of determination; *R*, ratio of mass of catalyst to volume of MO solution; *k*, kinetics constant; *t*, time of reaction.

* Corresponding author. Tel.: +54 114 964 8263; fax: +54 114 964 8263.
E-mail address: vcdall@ffyb.uba.ar (V. Campo Dall' Orto).

0926-3373/$ – see front matter © 2008 Elsevier B.V. All rights reserved.
doi:10.1016/j.apcatb.2008.01.030

combination with a catalyst and/or UV light to produce free radical intermediates. The hydroxyl radical is one of the main species that react with non-saturated organic compounds leading to either partial or complete degradation.

Electron spin resonance (ESR) spectroscopy is a useful method for the detection of paramagnetic complexes and relatively stable free radicals. Nevertheless, free radicals with very short half-lives can be detected using spin trap techniques and ESR. The spin trap 5,5-dimethyl-1-pyrroline-*N*-oxide (DMPO) allows the detection of hydroxyl radicals (DMPO/$^{\bullet}$OH), superoxide radicals (DMPO/$O_2^{\bullet-}$) and carbon-centered radicals (DMPO/$^{\bullet}$C) [12,13].

Fenton reagent is a combination of Fe(III)/H_2O_2 employed in the oxidation of aromatic hydrocarbons and phenols, but only effective under acidic conditions [14–16]. Cu(II) can also be used with hydrogen peroxide for similar applications in a wider pH range. The catalytic activity of copper ion in peroxide activation to give hydroxyl radical is dramatically enhanced by complexation with pyridine, organic acids, amino acids and other chelating agents, but the recovery of these compounds is expensive since they are all soluble in water [17–20].

The heterogeneous catalysts are an interesting alternative that combine effectiveness in dye decolorization with ease of recovery. These materials behave differently from homogeneous catalysts since parallel processes (i.e. activation of the oxidant, adsorption of the substrate) and consecutive reactions take place when two phases are involved.

Transition metal ions supported by alumina and silica have been found to be more effective for peroxide decomposition than homogeneous catalysts [21,22] and copper complexes of alumina have been used for color removal from waste water [23,24]. In addition, the hydroxylation of phenols by H_2O_2 has been tested using Cu(II)-salicylaldimine complexes immobilized on silica particles as catalysts [25].

Chitosan, a functionalized, non-soluble polymer combined with Cu^{2+} and H_2O_2 has been employed for degradation of antraquinone textiles and azo dyes [26].

In this work, we explored the application of a new heterogeneous catalyst for H_2O_2 activation and the degradation of Methyl Orange, an azo dye. The polymeric synthetic material [poly(EGDE-MAA-2MI)] with the characteristics of a polyampholyte was synthesized from ethylene glycol diglycidyl ether (EGDE), methacrylic acid (MAA) and 2-methylimidazole (2MI) [27], and the complex with copper ion was obtained [28].

Kinetic studies of H_2O_2 activation, degradation of the dye and parallel adsorption to the polymer were carried out to evaluate the performance and the efficiency of Cu(II)-poly(EGDE-MAA-2MI).

2. Experimental procedures

2.1. Preparation and characterization of complexes

The new polyampholyte was synthesized according to previous reports [27]. Cu(II)-poly(EGDE-MAA-2MI) was prepared with 0.100 g of polyampholyte and 2.0 mL of $CuSO_4$ solution in deionized water in two concentration levels: 25 and 80 mM. Then the samples were centrifuged and filtered after 48 h of contact time [28].

Free Cu(II) concentration in supernatant solutions could be determined spectrophotometrically since $Cu(NH_3)_4^{2+}$ (formed by ammonium hydroxide addition) absorbs radiation at 640 nm.

The nitrogen adsorption isotherm was collected at 77 K on a Micromeritics Gemini 2360 system. Specific surface area was calculated using the BET (Brunauer–Emmett–Teller) equation.

The continuous-wave (CW) electron spin resonance (ESR) spectra of Cu(II)-poly(EGDE-MAA-2MI) were obtained at 20 °C using an X-band CW ESR Spectrometer Bruker ECS 106 (Bruker Instruments, Inc., Berlin, Germany). The spectrometer settings were: center field: 3300 G, sweep width: 1200 G, microwave power: 10 mW, microwave frequency: 9.75 GHz, conversion time: 5.12 ms, time constant: 5.12 ms, modulation frequency: 50 KHz, modulation amplitude: 0.107 G, gain: 2.00×10^2, resolution: 1024 points. All spectra were the accumulation of 100 scans.

Simulated spectra were obtained by the calculation of the quantum density matrix using the Liouville equation with the incorporation of the modulated Zeeman effect [29,30]. Molar proportion yields and coupling constants were calculated from the simulated spectra.

Scanning electron microscopy (SEM) imaging was carried out with a scanning electron microscope Field Emission SEM (Zeiss Gemini DSM 982) operated at a 0.3 kV acceleration voltage.

2.2. Measurements of hydrogen peroxide and free radicals

The measurements of the concentration of H_2O_2 as a function of time were made for a mixture of 10.0 mg of 806 μmol g^{-1} (926 μmol m^{-2}) Cu(II)-poly(EGDE-MAA-2MI) with 10.0 mL of 0.1 mM hydrogen peroxide in 0.1 M phosphate buffer pH 7.0 for a period of 45 min. The concentration of hydrogen peroxide was estimated with xylenol orange and sorbitol, according to the method described by Wolf [31].

Free radical generation was followed as a function of time by spin trapping and CW ESR detection. The spin trap was 5,5-dimethyl-1-pyrroline-*N*-oxide (DMPO; SIGMA, USA). Catalytic systems for ESR experiments were prepared with 10.0 mg of 806 μmol g^{-1} (926 μmol m^{-2}) Cu(II)-poly(EGDE-MAA-2MI) and 10.0 mL of 11 mM H_2O_2 solution in deionized water. Then 80-μL aliquots taken at different contact times from 0 to 60 min were mixed with 40-μL aliquots of 1 M DMPO, and CW ESR spectra of the DMPO spin adducts were recorded at 3 min after incubation at 20 °C.

The spectrometer settings were: center field: 3483 G, sweep width: 80 G, microwave power: 10 mW, microwave frequency: 9.75 GHz, conversion time: 2.56 ms, time constant: 2.56 ms, modulation frequency: 50 KHz, modulation amplitude: 0.107 G, gain: 2.00×10^4, resolution: 1024 points. All spectra were the accumulation of 10 scans. DMPO adduct signal intensities were measured as the total height of the second field peak in the respective CW ESR spectra [32]. Since the ESR spectra had equivalent line-shapes and line-widths at different

times, the signal intensities were proportional to the radical concentrations. Then, the adduct yields were estimated from the total heights of the respective peaks. The adduct yield is the amount accumulated in a fixed time.

The 4-aminoantipyrine reaction [33] was performed mixing 2.0 mL of reagent solution, 10.0 mL of test solution and 10.0 mg of the Cu(II)-polyampholyte (or non-complexed polyampholyte). The absorbance of the solution was read as a function of time at 505 nm. The reagent was prepared with 2 g of phenol, 40 mg of 4-aminoantipyrine and 0.1 M phosphate buffer pH 7.0 up to 100 mL.

2.3. Catalytic system

The kinetics of the reaction of Methyl Orange (MO) with H_2O_2 in the presence of Cu(II)-poly(EGDE-MAA-2MI) was followed by monitoring the decay of the absorbance at 464 nm as a function of time in 0.1 M phosphate buffer pH 7.0. The system was also tested in 0.1 M acetic acid/acetate buffer pH 4.0.

The Cu(II)-poly(EGDE-MAA-2MI) complex was stable at pH 7.0 in 0.1 M phosphate buffer, but the solutions of $CuSO_4$ were made in deionized water. Phosphate buffer was also used with other organic complexes of copper ion [17] without problems of interference.

Two catalysts were used:

- Catalyst A was Cu(II)-poly(EGDE-MAA-2MI) with 480 μmol of copper ion per gram of polymer or 696 μmol - per m^2 of surface area.
- Catalyst B was Cu(II)-poly(EGDE-MAA-2MI) with 806 μmol of copper ion per gram of polymer or 926 μmol - per m^2 of surface area.

The ratio (R) of mass of catalyst (mg) to volume of MO solution (mL) was varied between 0.25 and 5.00.

All the experiments were performed at 20.0 ± 0.5 °C.

The double exponential decay with five parameters was selected as the best empirical equation to describe the complete process of decolorization of MO in the presence of H_2O_2 and the catalyst. The value of the coefficient of determination ($\mathbf{R}^2$) for the non-linear regression was taken into account for this selection, which was higher than 0.99 in all the experiments. This model was compared with single exponential decay with two and three parameters ($\mathbf{R}^2 < 0.96$).

For the control of dye adsorption at pH 7.0 in the absence of H_2O_2, double exponential decay with four parameters for catalyst A and single exponential decay with three parameters for catalyst B were also selected with the $\mathbf{R}^2$ criteria.

The stability of the catalysts A and B as a function of the initial concentration of hydrogen peroxide ($[H_2O_2]_0$) was evaluated in a concentration range between 25 and 100 mM for $R = 2.50$. The catalysts were reused three times for each concentration level of H_2O_2. The absorbance of 40 μM MO was measured during the reaction and the plots of each cycle were compared to determine if the performance of the catalyst had been affected.

The FTIR spectra of the catalysts in previous contact with 50 mM $[H_2O_2]_0$ were recorded both before and after the experiments to detect structural changes. They were recorded on a Spectrum 1000 PerkinElmer spectrometer using KBr pellets. The material was dried and placed in a desiccator at 20 °C prior to pellet preparation.

The adsorption isotherms were obtained for MO at pH 7.0 in a concentration range between 10 and 500 μM, and $R = 1.00$. FTIR spectra of the MO adsorbed on the catalyst surface were recorded.

3. Results and discussion

3.1. Characterization of the heterogeneous catalyst

The new polymer was synthesized via reaction of ethylene glycol diglycidyl ether (EGDE), methacrylic acid (MAA) and 2-methylimidazole (2MI) in the presence of benzoyl peroxide [27]. Scheme 1 shows the chemical structure for poly(EGDE-MAA-2MI). The specific surface area for the Cu(II)-complexes was 0.69 and 0.87 $m^2\ g^{-1}$ for the catalyst A and B, respectively in concordance to the network expansion observed in the non-complexed polyampholyte (0.6 $m^2\ g^{-1}$) [27].

This material offers the versatility of complex copper ions due to the presence of the imidazole ligand and the carboxylate,

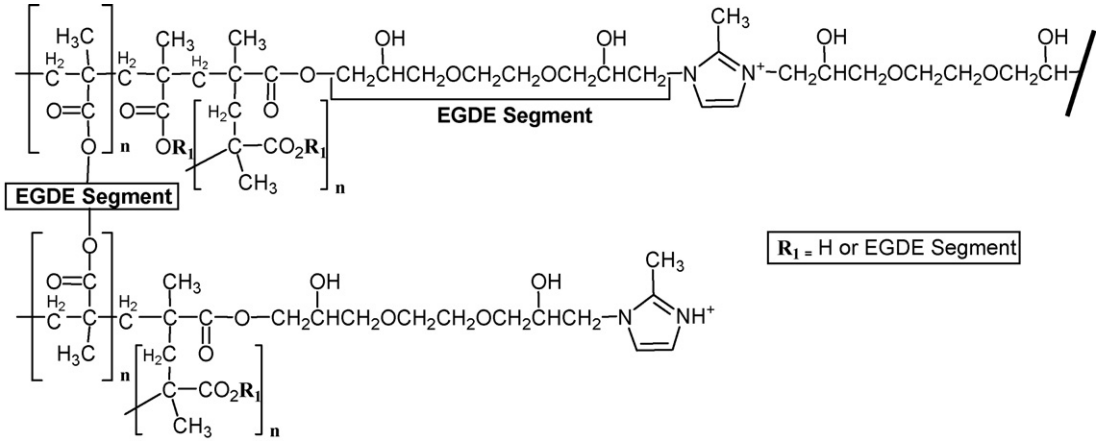

Scheme 1. Structure of poly(EGDE-MAA-2MI).

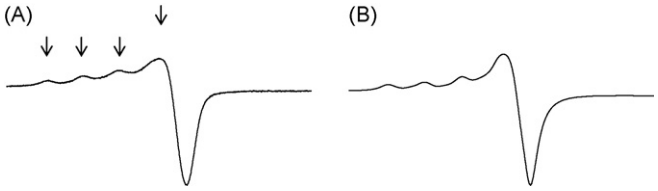

Fig. 1. Experimental (A) and simulated (B) CW ESR in band X spectra of the solid Cu(II)-poly(EGDE-MAA-2MI) complex recorded at room temperature. The arrows in spectrum A indicate the well-resolved hyperfine structure of the ESR signal due to the copper nuclei.

with a maximum loading capacity of 9.0×10^{-4} mol Cu(II) per gram of polyampholyte [28].

The complex was also studied by ESR. Fig. 1 shows the experimental and simulated spectra of the solid Cu(II)-poly(EGDE-MAA-2MI) complex at room temperature.

The simulated spectrum was obtained according to a spin Hamiltonian ($\hat{H}$) with an axial symmetry. The $a_{||}$ and $a_{\perp}$ values obtained from simulation and fits of the solid Cu(II)-poly(EGDE-MAA-2MI) complex spectrum, at room temperature, were 145 and 10 G, respectively [29,30].

The slight discrepancy in the simulated spectrum can be due to the existence of two or more paramagnetic species in the Cu(II)-poly(EGDE-MAA-2MI) complex.

The first conclusion from the ESR spectrum is that the paramagnetic entities in the solid complex are isolated Cu(II) with a well resolved hyperfine structure in which the copper may be coordinated to the nitrogen of the imidazole and/or the oxygen of the carboxylate in agreement with previous FTIR studies [28]. Fig. 1A shows the characteristic axial spectrum of a mononuclear square-planar copper(II) species.

SEM is widely used to study the morphological features and surface characteristics of the adsorbent materials [34]. In the present study, SEM images were used to evidence the adsorption of MO around the surface of the catalyst by comparison with the unloaded catalyst (Fig. 2).

3.2. Hydrogen peroxide activation mechanism

When a solution of MO was mixed with H_2O_2 practically no changes were observed in color intensity. After the addition of Cu(II)-poly(EGDE-MAA-2MI) the release of gas was followed by color removal of the dye. The results depicted in Fig. 3 indicate that this system acts as an efficient heterogeneous catalyst of hydrogen peroxide degradation followed by decolorization, and the dye adsorbs to the polymer to some extent.

A possible mechanism of interaction between the peroxide and the catalyst involves H_2O_2 bound in a coordination site of

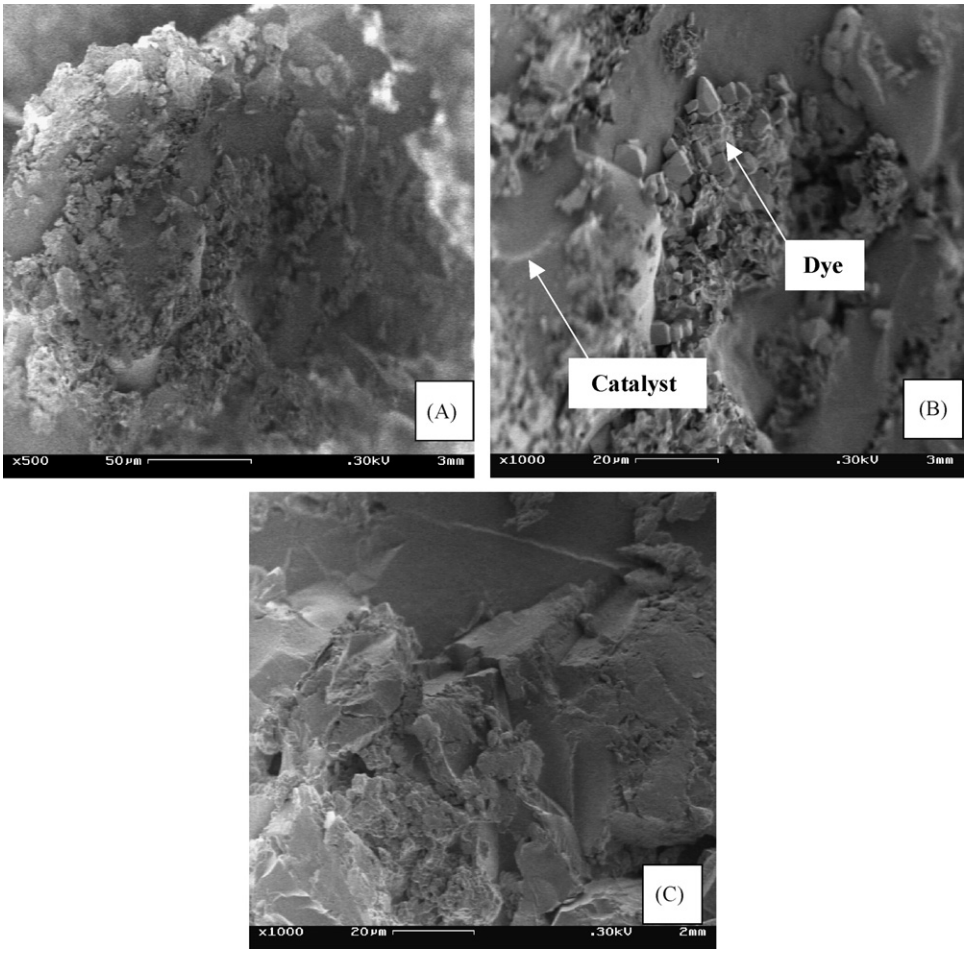

Fig. 2. SEM images for the Methyl Orange adsorbed to the surface of the catalyst at different magnification ranges [A and B] and the unloaded catalyst [C].

Cu(II) in the place of a water molecule [35]. The formed complex between Cu(II)-poly(EGDE-MAA-2MI) and superoxide reacts with another H_2O_2 molecule to give dioxygen, hydroxyl radical and water. Then the Cu(II)-poly(EGDE-MAA-2MI) is regenerated by H_2O_2 producing more $^{\bullet}OH$.

$$\begin{aligned}
&\text{L-Cu}^{2+} + H_2O_2 \longrightarrow \text{L-Cu}^{+\bullet}O_2H + H^+\\
&\text{L-Cu}^{+\bullet}O_2H + H_2O_2 \longrightarrow \text{L-Cu}^{+} + O_2 + {}^{\bullet}OH + H_2O\\
&\text{L-Cu}^{+} + H_2O_2 \longrightarrow \text{L-Cu}^{2+} + {}^{\bullet}OH + OH^-\\
&\overline{3\,H_2O_2 \longrightarrow O_2 + 2\,{}^{\bullet}OH + 2\,H_2O}
\end{aligned}$$

The 806 μmol g^{-1} (926 μmol m^{-2}) Cu(II)-poly(EGDE-MAA-2MI) was tested for its catalytic activity towards the decomposition of hydrogen peroxide in 0.1 M phosphate buffer pH 7.0 for a period of 45 min. As expected, the reaction followed a third-order kinetics according to the integrated rate expression:

$$k = \frac{1}{2 \times t} \times \left[\frac{1}{[H_2O_2]^2} - \frac{1}{[H_2O_2]_0} \right] \quad (1)$$

where $[H_2O_2]_0$ and $[H_2O_2]$ are the initial and intermediate hydrogen peroxide concentrations, t is the reaction time, k is the third-order rate constant calculated by linear regression ($\mathbf{R} > 0.99$) to be 1.26×10^4 mol^{-2} dm^6 s^{-1} for 0.1 mM $[H_2O_2]_0$, with a $t_{1/2}$ of 3.3 h. For higher amounts of initial hydrogen peroxide a departure from this empirical model was observed.

The production of free radicals that diffuse into the solution was confirmed by spin trapping experiments with DMPO. Fig. 4 shows the CW ESR spectra produced by aliquots of supernatant from the heterogeneous system Cu(II)-poly(EGDE-MAA-2MI)/H_2O_2 in the presence of DMPO spin trap. The simulation and fits of the experimental spectra allowed establishing the presence of three species: a DMPO/$^{\bullet}$OH adduct (I), a DMPO/$^{\bullet}$Carbon centered radical adduct (II) and a nitroxide-like radical (III),

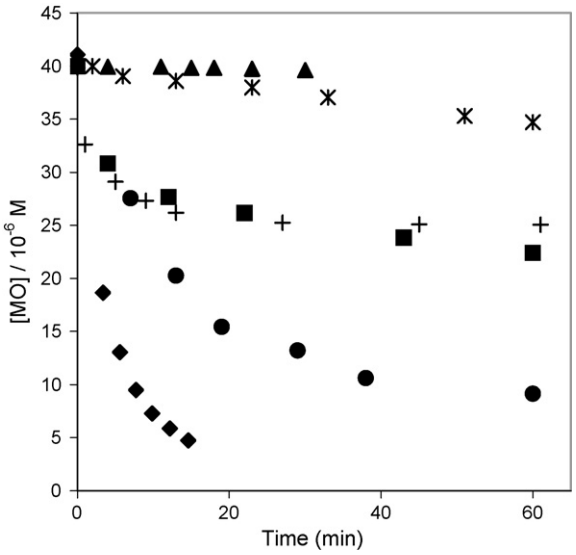

Fig. 3. Evolution of 40 μM $[MO]_0$ under different experimental conditions. In contact with: 240 mM $[H_2O_2]_0$ (▲); 240 mM $[H_2O_2]_0$ and 1.2 mM Cu(II) (*); 240 mM $[H_2O_2]_0$ and poly(EGDE-MAA-2MI) $R = 2.50$ (■). In contact with 480 μmol g^{-1} Cu(II)-poly(EGDE-MAA-2MI) $R = 2.50$ and 24 mM $[H_2O_2]_0$ (◆); 2.4 mM $[H_2O_2]_0$ (●); 0 mM $[H_2O_2]_0$ (+).

possibly a DMPO semi-oxidation product [36]. Table 1 shows the hyperfine interaction constant values for the three species.

In these experimental conditions the DMPO/$^{\bullet}$Carbon centered radical adduct and the nitroxide-like radical presented a transient kinetic behavior.

The molar fraction of the DMPO/$^{\bullet}$OH adduct was higher than 0.70 measured beyond 10 min after the addition of H_2O_2, and it presented a maximum at 40 min (Fig. 5).

Fig. 6 shows the ESR spectra at X band produced by aliquots of supernatant from the heterogeneous system Cu(II)-poly(-

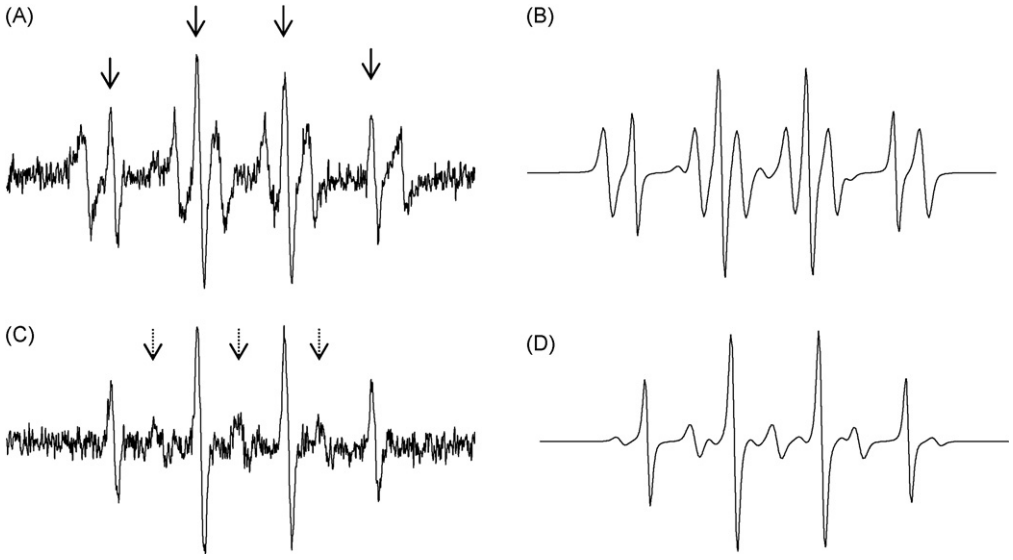

Fig. 4. Experimental (A and C) and simulated (B and D) CW ESR in band X spectra from spin trapping experiments with DMPO. Heterogeneous system: Cu(II)-poly(EGDE-MAA-2MI)/H_2O_2; contact time: 5 min (A) and 10 min (C). The continuous arrows in spectrum A indicate the lines corresponding to the hyperfine splitting of DMPO/$^{\bullet}$OH adduct. The segmented arrows in spectrum C indicate the lines corresponding to the hyperfine splitting of the nitroxide-like radical. The molar fractions of DMPO/$^{\bullet}$OH adduct, DMPO/$^{\bullet}$Carbon centered radical adduct and nitroxide-like radical were 0.37, 0.59, 0.04 and 0.70, 0.10, 0.20 in spectra A and C, respectively.

Table 1
Hyperfine interaction constant values for the DMPO/•OH adduct, the DMPO/•Carbon centered radical adduct and the nitroxide-like radical

Radical	a_N (G)	$a_{H\beta}$ (G)
DMPO/•OH	14.98	14.59
DMPO/•Carbon centered radical	15.59	22.78
Nitroxide-like radical	14.00	–

The data were obtained by simulation and fits of the experimental spectra.

EGDE-MAA-2MI)/deionized water in the presence of DMPO spin trap.

In these experimental conditions, the DMPO/•Carbon centered radical adduct was the predominant species with a molar fraction higher than 0.93 measured at a contact time of 5 min. The DMPO/•OH concentration was negligible. The 4-aminoantipyrine reaction (Fig. 7) [37] brought another evidence of the generation of free radicals.

This last ESR response cannot be a consequence of the activation of dissolved dioxygen by trace amounts of Cu(I) because the autoxidation of Cu(I) proceeds with release of H_2O_2 [38–40]. In such a case the signal due to DMPO/•OH should have been present.

A solution of 2.5 mM Cu(II) gave negative results for 4-aminoantipyrine reaction and generated a weak ESR signal of •OH. In this sense, we can say that the responses seen in Fig. 6 were not induced by free Cu(II).

3.3. Decolorization of Methyl Orange (MO)

3.3.1. General aspects

The oxidative catalytic activity of the copper complex was tested using the azo-based dye Methyl Orange as a model compound. The variables studied were copper content, ratio of mass of catalyst to volume of MO solution (R) and initial concentration of H_2O_2 ($[H_2O_2]_0$).

The Cu(II)-poly(EGDE-MAA-2MI)/H_2O_2 system was highly efficient in the decolorization of this dye. Without the polyampholyte, the Cu(II)/H_2O_2 system only oxidized less than 10% of the compound at the time that almost complete decolorization was reached with the new catalyst and lower amounts of H_2O_2 (Fig. 3).

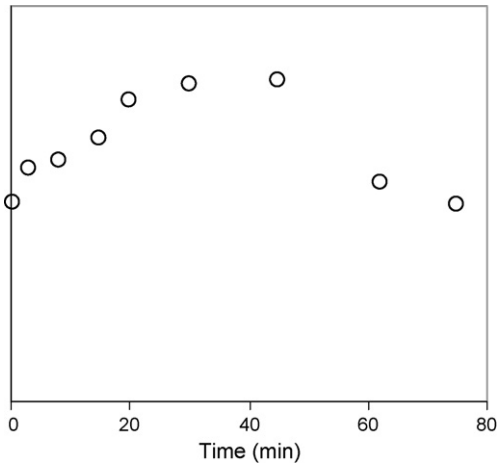

Fig. 5. Concentration profile of DMPO/•OH adduct (expressed in arbitrary units) produced by Cu(II)-poly(EGDE-MAA-2MI)/H_2O_2.

The system was tested at pH 4.0 and 7.0, being more effective in the latter. The subsequent experiments were performed under this condition.

The overall process of dye removal from the solution has a complex description involving surface adsorption and oxidative degradation. Both adsorbed and soluble MO molecules can be oxidized by the free radicals formed from H_2O_2 but the bound fraction resulted to be more stable, as it will be seen in this section.

The kinetic profiles of MO removal for poly(EGDE-MAA-2MI) in contact with H_2O_2 and for Cu(II)-poly(EGDE-MAA-2MI) in absence of H_2O_2 were compared in Fig. 3. Besides, the concentration of the dye evolves in the same way in presence or in absence of H_2O_2 for poly(EGDE-MAA-2MI). From these results it can be concluded that the decrease of MO concentration was due to a process of adsorption on the surface of the particles in both cases. Even if the dye has negative charge at pH 7.0 (pK_a 3.7) we can infer that it did not bind electrostatically to the immobilized Cu(II) because these profiles of concentration were similar.

At pH 7.0 the polyampholyte exhibited negative net charge with negative domains due to carboxylate groups and positive domains from 2-methylimidazolium residues; Cu(II) only occupied 32% of the total binding sites at saturating conditions, leaving free functional groups for dye adsorption.

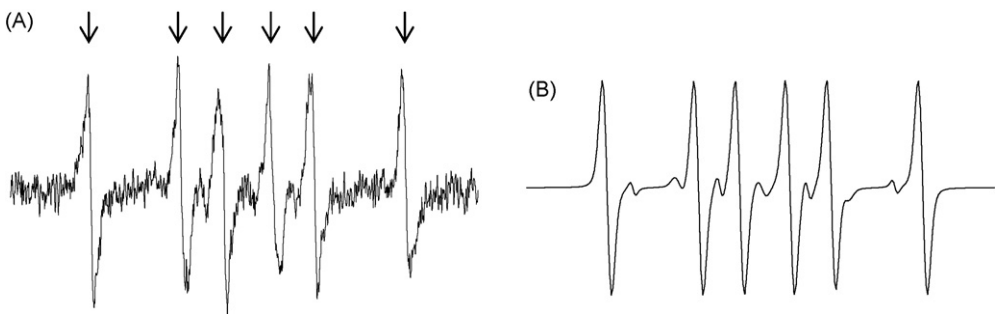

Fig. 6. Experimental (A) and simulated (B) CW ESR in band X spectra from spin trapping experiments with DMPO. Heterogeneous system: Cu(II)-poly(EGDE-MAA-2MI)/deionized water; contact time: 5 min. The arrows in spectrum A indicate the lines corresponding to the hyperfine splitting of DMPO/•Carbon centered radical adduct. The molar fractions of DMPO/•OH adduct, DMPO/•Carbon centered radical adduct and nitroxide-like radical were 0.03, 0.93 and 0.04 in spectra A, respectively.

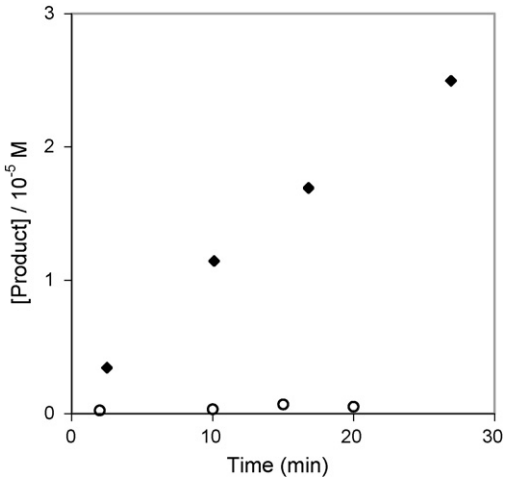

Fig. 7. 4-Aminoantipyrine reaction for Cu(II)-poly(EGDE-MAA-2MI) (◆), and for poly(EGDE-MAA-2MI) (○) in contact with deionized water.

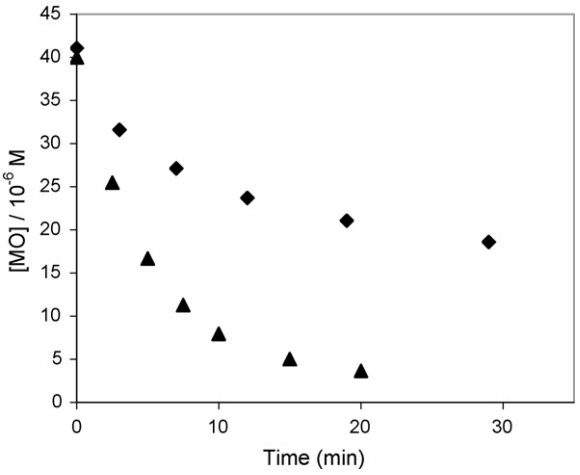

Fig. 9. Evolution of 40 μM $[MO]_0$ in contact with 24 mM $[H_2O_2]_0$ and $R = 1.00$ of: 480 μmol g^{-1} Cu(II)-poly(EGDE-MAA-2MI) (◆) and 806 μmol g^{-1} Cu(II)-poly(EGDE-MAA-2MI) (▲).

The MO molecules can compete with copper ions for 2MI sites on the particles. In this sense, free Cu(II) content in the solutions at the end of the reaction was below 0.1 mM in all cases.

3.3.2. Empirical kinetic model for evolution of MO concentration ([MO])

The concentration of MO in the reaction with hydrogen peroxide exhibited an exponential decay according to the empirical kinetic expression (2). This equation fitted well with the experimental results obtained during the first 90 min of reaction.

$$[MO] = [MO]_{\infty} + [MO]_{ads} \times e^{-k_1 xt} + [MO]_{deg} \times e^{-k_2 xt} \quad (2)$$

$[MO]_{\infty}$ represents the free MO that decomposed with a very low kinetic constant since a complete removal was observed after 24 h. The second term represents the dye adsorption to the polymeric complex, and the third term involves the degradation.

$[MO]_{ads}$ is the total amount of MO per liter of solution that will be removed by adsorption. $[MO]_{deg}$ is the total amount of MO per liter of solution that will be removed by degradation.

In general, the adsorbed MO was observed on the surface of the particles after the mentioned period of time. Thus, it was evidently more stable than in solution. Nevertheless, it would eventually be degraded by oxidation if kept in contact with the rest of peroxide for a longer period of time.

3.3.3. Effect of the initial MO concentration ($[MO]_0$)

The kinetic constant for degradation (k_2) is a pseudo-first-order parameter not affected by $[MO]_0$. The amount of dye decomposed by action of H_2O_2 was proportional to $[MO]_0$.

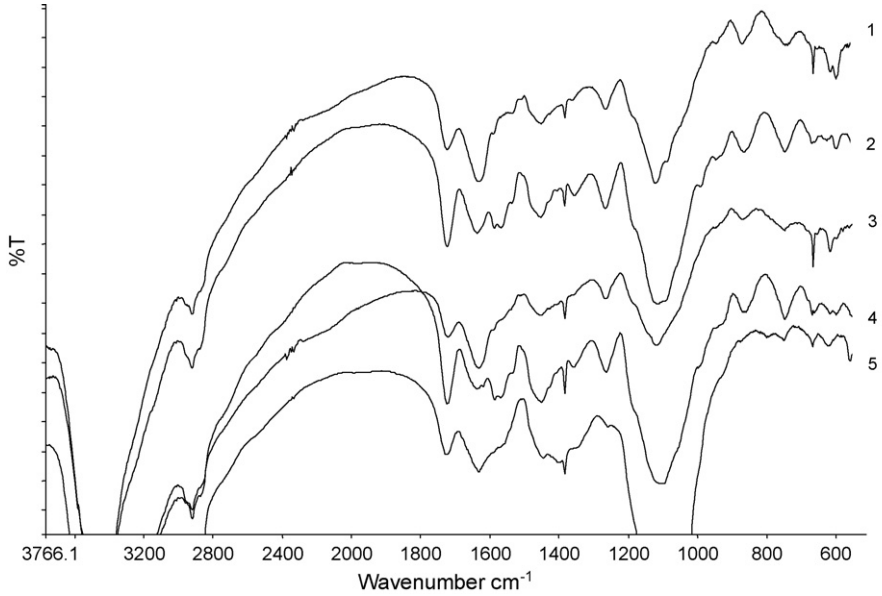

Fig. 8. FTIR spectra of: 806 μmol g^{-1} Cu(II)-poly(EGDE-MAA-2MI) before [1] and after contact with 50 mM $[H_2O_2]_0$ [2]; 480 μmol g^{-1} Cu(II)-poly(EGDE-MAA-2MI) before [3] and after contact with 50 mM $[H_2O_2]_0$ [4]; 806 μmol g^{-1} Cu(II)-poly(EGDE-MAA-2MI) with adsorbed MO [5].

3.3.4. Effect of the initial H_2O_2 concentration ($[H_2O_2]_0$)

k_2 and $[MO]_{deg}$ increased with initial H_2O_2, working at a fixed $[MO]_0$ and a fixed R (Fig. 3).

The catalyst was stable for $[H_2O_2]_0$ up to 50 mM. Moreover, the performance in terms of degradation is known to be affected at hydrogen peroxide concentrations higher than 50 mM due to the hydroxyl radical scavenging effect. In fact, H_2O_2 can combine with $^{\bullet}OH$ producing $HO_2^{\bullet}$ with a smaller oxidation potential and reducing the probability of attack to organic molecules [41].

The FTIR spectra of the catalysts both before and at the end of the degradation of MO are shown in Fig. 8. There were non-significant structural changes after three cycles of reaction at the initial H_2O_2 concentration employed, and the efficiency of catalysis was preserved.

Nevertheless, the carboxylate stretching band at 1570 cm^{-1} increased after catalysis due to the pH value of the medium of reaction (7.0), as can be seen in spectra 2 and 4 (Fig. 8). When the complexes between copper ion and poly(EGDE-MAA-2MI) were synthesized, this band from carboxylate was either absent or the intensity was lower (spectra 1 and 3, Fig. 8). In that case, the H^+ from $2MIH^+$ in the native polyampholyte had been exchanged by Cu(II) and the pH had decreased and caused the partial protonation of free carboxylate.

3.3.5. Effect of copper ion content and the ratio of catalyst to dye solution (R)

The content of Cu(II) was varied in the polymer. Catalyst A had 480 μmol g^{-1} (696 μmol m^{-2}) Cu(II)-poly(EGDE-MAA-2MI), and catalyst B had 806 μmol g^{-1} (926 μmol m^{-2}) Cu(II)-poly(EGDE-MAA-2MI).

Besides, it was observed that the dye adsorbed on the particles of the catalyst to some extent when the reactions were made with either low $[H_2O_2]_0$ or low R. So the ratio (R) of mass of catalyst to volume of MO solution was introduced as a variable to follow the process of adsorption.

The preliminary results showed that catalyst B was more efficient for MO removal from the solution at a given $[H_2O_2]_0$, taking into account both adsorption and degradation (Fig. 9).

Fig. 10 exhibits the evolution of MO in the solution put in contact with Cu(II)-poly(EGDE-MAA-2MI)/H_2O_2 for 41 μM $[MO]_0$ and for different R, under conditions where both adsorption and degradation of the dye took place simultaneously in most cases. Table 2 presents the kinetic parameters from the fitting procedure for Eq. (2).

k_2 can be described by the following equation:

$$k_2 = k_{deg} \times [Cu^{2+}]^n \quad (3)$$

where n is the reaction order. A second-order dependence on the concentration of Cu(II) was found in the mixture for $R \leq 2.50$ and for both catalysts.

k_2 was assigned for the decomposition process because it increased together with $[MO]_{deg}$ as a function of $[H_2O_2]_0$, and it was lower than k_1 in all cases. The degradation of MO was expected to be slower than the adsorption. The overall dye adsorption process only involves mass transport and non-covalent bond formation. Instead, the degradation process involves mass transport of H_2O_2 to the catalyst, free radical formation on the catalytic surface, mass transport of reactants and the chemical reaction of oxidation of the dye.

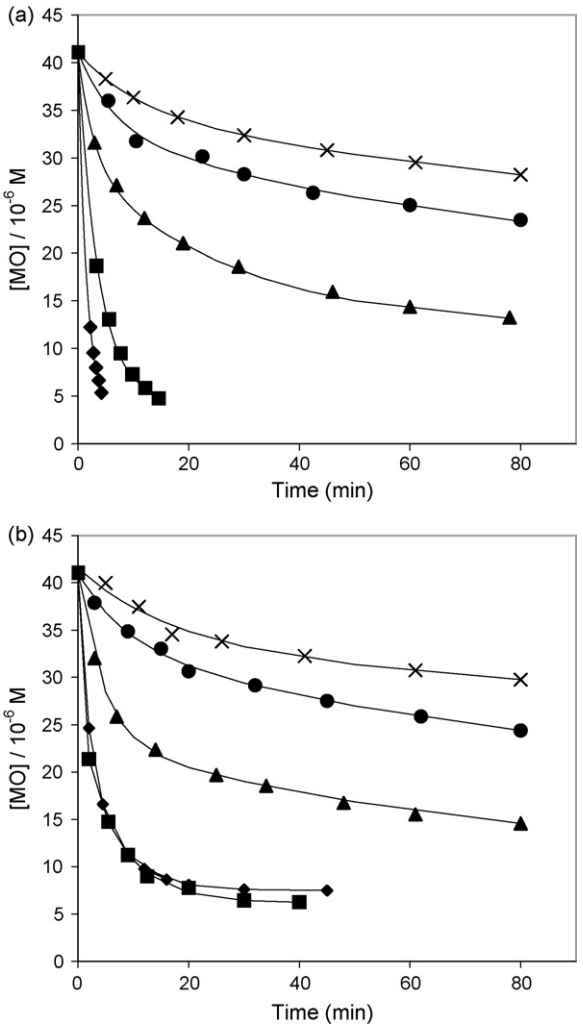

Fig. 10. (a) Evolution of 41 μM $[MO]_0$ in contact with 24 mM $[H_2O_2]_0$ and 480 μmol g^{-1} Cu(II)-poly(EGDE-MAA-2MI) for R: 0.25 (×); 0.50 (●); 1.00 (▲); 2.50 (■); 5.00 (◆). (b) Evolution of 41 μM $[MO]_0$ in contact with 11 mM $[H_2O_2]_0$ and 806 μmol g^{-1} Cu(II)-poly(EGDE-MAA-2MI) for R: 0.25 (×); 0.50 (●); 1.00 (▲); 2.50 (■); 5.00 (◆).

The kinetic constant for MO adsorption (k_1) is also a pseudo-first-order parameter that presented a second-order dependence on R (at limited ranges) for both catalysts, with a coefficient of determination higher than 0.999.

For catalyst A and 24 mM $[H_2O_2]_0$, a single exponential decay fitted well the experimental results at $R \geq 2.50$ because the adsorption became negligible. In fact, both adsorption and decomposition of MO should be enhanced with an increase in R, so a competition was established and degradation prevailed under these experimental conditions. $[MO]_{deg}$ increased and $[MO]_{\infty}$ decreased with R.

For catalyst B and 11 mM $[H_2O_2]_0$, k_2 reached a plateau at $R \geq 2.50$, limited by $[H_2O_2]_0$. The low $[H_2O_2]_0$ determined that $[MO]_{deg}$ kept stable in the whole R range and $[MO]_{ads}$ increased

Table 2
Non-linear regression parameters for different R

R	Cu in mixture (mM)	$[MO]_\infty$ (μM)	$[MO]_{ads}$ (μM)	$k_1/10^{-3}$ s^{-1}	$[MO]_{deg}$ (μM)	$k_2/10^{-3}$ s^{-1}
(a) Catalyst A and 24 mM $[H_2O_2]_0$						
0.25	0.12	20.3	6.0	1.55	14.7	0.130
0.50	0.24	17.3	8.6	2.5	15.2	0.19
1.00	0.48	12.1	11.5	6.0	17.4	0.57
2.50	1.20	4.5	–	–	36.5	4.5
5.00	2.40	2.8	–	–	38.2	10.4
(b) Catalyst B and 11 mM $[H_2O_2]_0$						
0.25	0.20	16	8	0.95	17	0.045
0.50	0.40	16	8	1.8	17	0.15
1.00	0.80	9.7	17.6	3.6	13.7	0.22
2.50	2.02	6.2	16.1	22	18.7	2.4
5.00	4.03	7.5	16.5	10	17	2.8
(c) Catalyst B and 24 mM $[H_2O_2]_0$						
1.00	0.80	3.0	–	–	37.0	3.3

Catalyst	$[H_2O_2]_0$ (mM)	k_{deg} (s^{-1} M^{-2})
(d) Kinetic constants (k_{deg}) for a second-order dependence on Cu(II) in mixture		
A	24	3.1×10^3 (SD: 1×10^2; $\mathbf{R}^2$: 0.9979)
B	11	5.9×10^2 (SD: 4×10^1; $\mathbf{R}^2$: 0.9926)
B	24	5.1×10^3

significantly for $R \geq 1.00$ with the consequent decrease in $[MO]_\infty$.

k_{deg} for catalyst B was higher than for catalyst A compared at the same $[H_2O_2]_0$ (Table 2), thus demonstrating that the catalytic efficiency is related to the content of copper ions.

As it can be observed, the combination of $R = 5.00$ for catalyst A with 24 mM $[H_2O_2]_0$ can led to >92% degradation of 41 μM MO in 10 min, avoiding the adsorption of the dye on the surface of the catalyst (Fig. 10 and Table 2). The combination of $R = 1.00$ for catalyst B with 24 mM $[H_2O_2]_0$ can led to >90% degradation of 40 μM MO in 20 min without adsorption (Fig. 9 and Table 2). Besides, the destruction of the catalyst by the deleterious action of the free radicals was prevented under these conditions.

Other copper-based heterogeneous catalysts require higher concentrations of hydrogen peroxide for complete degradation of azo dyes under similar experimental conditions [26], and higher temperatures [42,43].

Some carbon–Fe catalysts recently reported exhibit similar efficiency to this new material but restricted up to pH 3 and at 30 °C [44].

3.4. Dye adsorption in the absence of hydrogen peroxide

The FTIR spectrum 5 of Fig. 8 was obtained from MO adsorbed on catalyst B and it presented significant changes when compared with spectrum 1. The bands at 750 and 1570 cm^{-1} corresponding to the imidazole ring and carboxylate, respectively, were practically absent. This fact suggests that basic and acid groups from the catalyst could be involved in MO chemisorption (evidenced by SEM), even if MO has negative net charge at pH 7.0 and it is expected to interact mostly with $2MIH^+$. When hydrogen peroxide was added and the adsorbed MO was finally degraded, the absorption bands at 750 and 1570 cm^{-1} were recovered.

From this spectroscopic evidence we can say that the electrostatic interaction between negative MO and $2MIH^+$ is not the only mechanism of binding, and that π–π and hydrophobic interactions must also be taken into account.

The equilibrium of the dye adsorption to the surface of the heterogeneous catalysts was also studied (Fig. 11). The isotherms were L4-type in the classification of Giles et al. [45]. The first raise and plateau corresponded to the formation of the first ''monolayer''. Dyes can associate just before or after the moment of adsorption. In this case the ''layer'' consisted of isolated clusters or microcrystals of solute molecules adsorbed on a few of the most active sites (Fig. 2).

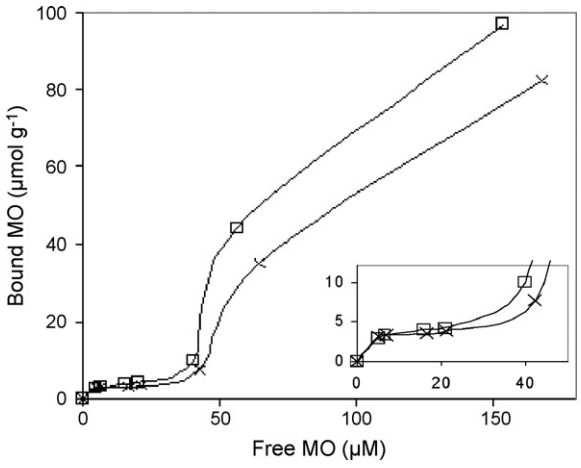

Fig. 11. Adsorption isotherms of MO on 480 μmol g^{-1} Cu(II)-poly(EGDE-MAA-2MI) (×) and 806 μmol g^{-1} Cu(II)-poly(EGDE-MAA-2MI) (□).

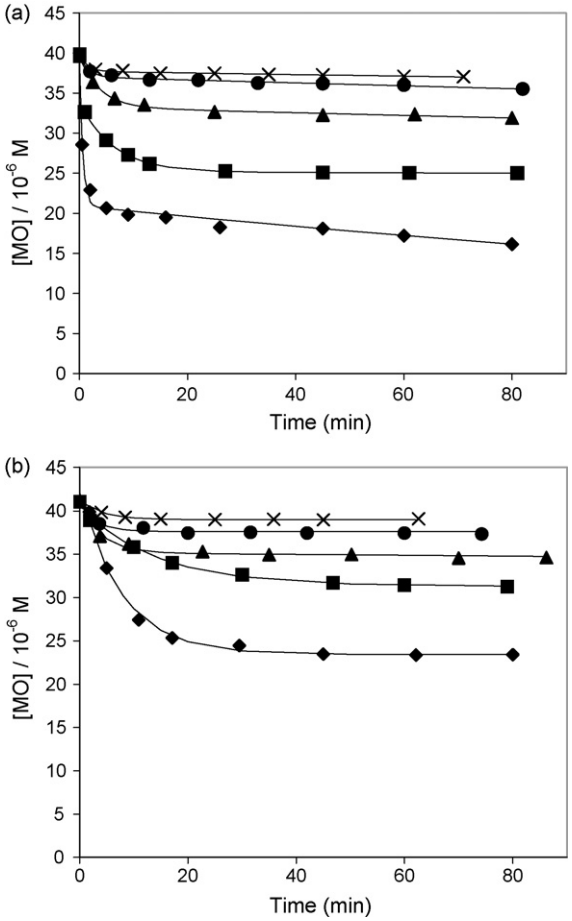

Fig. 12. (a) Evolution of 41 μM $[MO]_0$ in contact with 480 μmol g^{-1} Cu(II)-poly(EGDE-MAA-2MI) for *R*: 0.25 (×); 0.50 (●); 1.00 (▲); 2.50 (■); 5.00 (◆). (b) Evolution of 41 μM $[MO]_0$ in contact with 806 μmol g^{-1} Cu(II)-poly(EGDE-MAA-2MI) for *R*: 0.25 (×); 0.50 (●); 1.00 (▲); 2.50 (■); 5.00 (◆).

Then a second raise around 50–100 μM $[MO]_0$ indicated the complete saturation of the polymeric surface and the formation of a new surface of adsorption probably on top of the first because the polymeric network is non-porous and non-flexible. The isotherms rose steadily to a level representing adsorption several layers deep, involving strong interactions.

A third, significant raise (not shown) took place around 500 μM $[MO]_0$. At this concentration level the adsorption of ionic micelles of the dye should be considered.

The Langmuir model is only verified at $[MO]_0$ below 50 μM corresponding to the formation of the first ''layer'' of dye adsorbed on the polyampholyte. The parameters from the fitting procedure were: 3.8 and 4.9 μmol g^{-1} maximum loading capacity for catalyst A and B, respectively; and 1.3 and 3.1 μM dissociation constant for catalyst A and B, respectively. In fact, the amount of solute taken up at the first stage was much lower than the surface capacity. For catalyst B there is a total amount of 1.9 mmol of functional groups (free carboxylate, 2MI and $2MIH^+$) per gram of material. Supposing that carboxylate is close to 50%, then around 830 μmol of $2MIH^+$ per gram are exposed at pH 7.0.

All the kinetic experiments were performed in a sub-monolayer region.

Fig. 12 exhibits the evolution of 41 μM $[MO]_0$ at pH 7.0 in the absence of H_2O_2 when put in contact with Cu(II)-poly(EGDE-MAA-2MI) for different *R*.

The results fitted well to first-order kinetics with a double exponential decay and four parameters for catalyst A. One term corresponds to the MO fraction to be adsorbed on the non-occupied sites of the particles surface. The other term represents the free MO fraction that attaches with a very low kinetic constant, between 10^{-5} and 10^{-6} s^{-1}, probably on the previously formed clusters. The total amount of adsorbed MO increased and the total amount of ''free'' MO decreased in a linear way with *R*; the first-order kinetic constant for adsorption decreased with *R* except at $R = 5.00$.

The results for catalyst B fitted to a single exponential decay with three parameters. The exponential term represents the adsorption of MO and the non-dependent term is the free MO at equilibrium. The total amount of adsorbed MO increased and the amount of free MO decreased in a linear way with *R*.

As expected, if we compare the amount of free MO at equilibrium at pH 7.0 for both catalysts (Fig. 12), they are quite similar.

4. Conclusions

The Cu(II)-poly(EGDE-MAA-2MI) complex acted as a highly efficient heterogeneous catalyst in the degradation of H_2O_2 with decolorization of the azo-based dye Methyl Orange.

The complex combined effectiveness in dye decolorization and ease of recovery. The activation of the oxidant and the adsorption of the substrate were parallel processes that took place on the surface, both following pseudo-first-order kinetic profiles.

The formation of hydroxyl radicals was evidenced by ESR. The catalyst was stable at initial hydrogen peroxide concentrations up to 50 mM.

The efficiency of the catalyst increased with the amount of immobilized Cu(II). The kinetic constant for MO degradation at a given initial concentration of hydrogen peroxide followed a second-order dependence on copper ion content in the mixture.

Combining an adequate ratio of mass of complex to solution volume with 25 mM $[H_2O_2]_0$, an almost complete removal of the color was achieved between 10 and 20 min, in a neutral medium at room temperature with a minimal extension of adsorption to the catalytic surface.

Finally, the dye adsorbed on the polymer forming isolated aggregates evidenced by SEM. Other techniques such as ESR and FTIR contributed to enrich the study of the interaction between the dye and the catalyst.

Acknowledgements

Financial support from Universidad de Buenos Aires (UBACyT 04-07/B005, B037 and B062) and CONICET (PEI, Res. 1106/04; PIP 5021/05) are gratefully thanked. Juan Manuel Lázaro Martínez thanks CONICET for his doctoral fellowship. María Florencia Leal Denis thanks Universidad de Buenos Aires for her research fellowship for undergraduate students.

References

[1] S.-Y. Kim, J.-Y. An, B.-W. Kim, Dyes Pigments 76 (1) (2008) 256.
[2] J.H. Ramirez, F.J. Maldonado-Hódar, A.F. Pérez-Cadenas, C. Moreno-Castilla, C.A. Costa, L.M. Madeira, Appl. Catal. B 75 (3/4) (2007) 312.
[3] M. Janus, A.W. Morawski, Appl. Catal. B 75 (1/2) (2007) 118.
[4] H.-R. Kariminiaae-Hamedaani, A. Sakurai, M. Sakakibara, Dyes Pigments 72 (2) (2007) 157.
[5] G. Li, J. Qu, X. Zhang, H. Liu, H. Liu, J. Mol. Catal. A 259 (1/2) (2006) 238.
[6] Y. Yu, J.C. Yu, C.-Y. Chan, Y.-K. Che, J.-C. Zhao, L. Ding, W.-K. Ge, P.-K. Wong, Appl. Catal. B 61 (1/2) (2005) 1.
[7] A. Reife, H.S. Freeman, Environmental Chemistry of Dyes and Pigments, Wiley, New York, USA, 1996, pp. 3–41.
[8] N. Kannan, M.M. Sundaram, Dyes Pigments 51 (2001) 25.
[9] V. Meshko, L. Markovska, M. Mincheva, A.E. Rodrigues, Water Res. 35 (2001) 3357.
[10] I.D. Mall, V.C. Srivastava, N.K. Agarwal, I.M. Mishra, Chemosphere 61 (2005) 492.
[11] S.J.T. Pollard, G.D. Fowler, C.J. Sollars, R. Perry, Sci. Total Environ. 116 (1992) 31.
[12] Y. Mizuta, T. Masumizu, M. Kohno, A. Mori, L. Packer, Biochem. Mol. Biol. Int. 43 (5) (1997) 1107.
[13] S. Yue Qian, M.B. Kadiiska, Q. Guo, R.P. Mason, Free Radic. Biol. Med. 38 (1) (2005) 125.
[14] H.B. Dunford, Coord. Chem. Rev. 233/234 (2002) 311.
[15] N. Kang, D.S. Lee, J. Yoon, Chemosphere 47 (2002) 915.
[16] K. Nam, W. Rodriguez, J.J. Kukor, Chemosphere 45 (2001) 11.
[17] X.-G. Meng, J. Zhu, J. Yan, J.-Q. Xie, X.-M. Kou, X.-F. Kuang, L.-F. Yu, X.-C. Zeng, J. Chem. Technol. Biotechnol. 81 (2006) 2.
[18] T.-Y. Lin, C.-H. Wu, J. Catal. 232 (2005) 117.
[19] V. Shah, P. Verma, P. Stopka, J. Gabriel, P. Baldrian, F. Nerud, Appl. Catal. B 46 (2003) 287.
[20] F. Nerud, P. Baldrian, J. Gabriel, D. Ogbeifun, Chemosphere 44 (2001) 957.
[21] R.V. Prasad, N.V. Thakkar, J. Mol. Catal. 92 (1994) 9.
[22] R.N. Ram, B.B. Prasad, Z. Phys. Chem. 259 (1978) 1169.
[23] I.A. Salem, Appl. Catal. B 28 (2000) 153.
[24] A.H. Gemeay, M.A. Salem, I.A. Salem, Colloids Surf. A 117 (1996) 245.
[25] S. Ray, S.F. Mapolie, J. Darkwa, J. Mol. Catal. A 267 (2007) 143.
[26] R. Suláková, R. Hrdina, G.M.B. Soares, Dyes Pigments 73 (2007) 19.
[27] M.F. Leal Denis, R.R. Carballo, A.J. Spiaggi, P.C. Dabas, V. Campo Dall' Orto, J.M. Lázaro Martínez, G.Y. Buldain, React. Funct. Polym. 68 (2008) 169.
[28] J.M. Lázaro Martínez, M.F. Leal Denis, V. Campo Dall' Orto, G.Y. Buldain, Eur. Polym. J. 44 (2008) 392–407.
[29] M. Kälin, I. Gromov, A. Schweiger, J. Magn. Reson. 160 (2003) 166.
[30] D.E. Budil, S. Lee, S. Saxena, J.H. Freed, J. Magn. Reson. A 120 (1996) 155.
[31] S.P. Wolf, Methods Enzymol. 233 (1994) 182.
[32] D. Barr, J. Jiang, R.T. Weber, Experimental Techniques Note 3, Bruker Instruments, Inc., EPR Division, USA.
[33] M.B. Ettinger, C.C. Ruchhoft, R.J. Lishka, Anal. Chem. 23 (12) (1951) 1783–1788.
[34] S. Gupta, A. Pal, P.K. Ghosh, M. Bandyopadhyay, J. Environ. Sci. Health A 38 (2003) 381.
[35] L. Pecci, G. Montefoschi, D. Cavallini, Biochem. Biophys. Res. Commun. 235 (1997) 264.
[36] G.R. Buettner, Free Radic. Biol. Med. 3 (4) (1987) 259.
[37] M.B. Ettinger, C.C. Ruchhoft, R.J. Lishka, Anal. Chem. 23 (12) (1951) 1783.
[38] P.M. Hanna, R.P. Mason, Arch. Biochem. Biophys. 295 (1992) 205.
[39] M.R. Gunther, P.M. Hanna, R.P. Mason, M.S. Cohen, Arch. Biochem. Biophys. 316 (1995) 515.
[40] M.J. Burkitt, S.Y. Tsang, S.C. Tam, I. Bremmer, Arch. Biochem. Biophys. 323 (1995) 63.
[41] J. De Laat, T.G. Le, Appl. Catal. B: Environ. 66 (2006) 137.
[42] Z. Qiu, Y. He, X. Liu, S. Yu, Chem. Eng. Process. 44 (2005) 1013.
[43] N.N. Fathima, R. Aravindhan, J.R. Rao, B.U. Nair, Chemosphere 70 (2008) 1146.
[44] J.H. Ramirez, F.J. Maldonado-Hódar, A.F. Pérez-Cadenas, C. Moreno-Castilla, C.A. Costa, L.M. Madeira, Appl. Catal. B 75 (2007) 312.
[45] C.H. Giles, T.H. MacEwan, S.N. Nakhwa, D. Smith, J. Chem. Soc. (1960) 3973.